electrochem

MDPI

Article

Investigation of Physiochemical Impact of Organic Molecule L-Lysine on Ammonium Dihydrogen Phosphate Single Crystal for Optoelectronics Applications

Shruti Patle [1], Dinesh Rotake [2,*] and Kishor Rewatkar [3]

[1] Department of Applied Physics, Priyadarshini J. L. College of Engineering, Nagpur 440009, India
[2] Department of Electrical Engineering, Indian Institute of Technology, Hyderabad 500001, India
[3] Vidya Vikas Arts Commerce and Science College, Samudrapur 442305, India
* Correspondence: ee22pdf04@iith.ac.in

Abstract: Ammonium dihydrogen phosphate (ADP) single crystals along with the incorporated 0.5 and 1% L-lysine, an organic molecule which possesses a good nonlinear response, were grown with the vision to meet the requirements of the optoelectronic industry. The inclusion of the L-lysine molecule in the crystal was confirmed by the XRD and EDX. The experiment not only confirms the inclusion level of the impurity but also the capability of the amino acid molecule to bond hydrogen within the crystal facet. A minor decrease in lattice parameters was reported for all ADP: L-lysine crystals compared with pure ADP. The structures of the grown crystals were identified as tetragonal with the space group I42d by the single-crystal XRD analysis. Vibrational signatures and functional groups were confirmed using FTIR spectroscopy. The thermal stability and decomposition temperatures of 0.5 and 1% L-lysine-added crystals were measured by TG/DTA and found to be 203 °C and 207 °C, respectively. The UV–visible transmission spectra prove a higher transparency for doped crystals as compared to pure crystals; therefore, these doped crystals can be considered the best option for the frequency doubling process in a broad range of visible and near-IR spectra. The improved hardness of the doped crystals was confirmed by the Vickers hardness data. The nonlinear optical (NLO) behaviour investigated using a second-harmonic generation (SHG) technique, indicating an efficient quadratic nonlinear coefficient of ADP: Lysine crystals at a 1064 nm initial wavelength, shows about 1.5-fold higher efficiency compared with undoped ADP.

Keywords: NLO crystal; optoelectronics; TGA; microhardness; SHG efficiency

Citation: Patle, S.; Rotake, D.; Rewatkar, K. Investigation of Physiochemical Impact of Organic Molecule L-Lysine on Ammonium Dihydrogen Phosphate Single Crystal for Optoelectronics Applications. *Electrochem* **2023**, *4*, 255–272. https://doi.org/10.3390/electrochem4020017

Academic Editor: Masato Sone

Received: 18 February 2023
Revised: 13 April 2023
Accepted: 14 April 2023
Published: 24 April 2023

1. Introduction

Solids having a specific pattern of constituent arrangement that presents identical surroundings at every point and possesses no grain boundaries are termed single crystals. This special category of material offers many outstanding features applicable in optical, electronics and optoelectronic industries. In the past few decades, the optoelectronic branch of engineering has become of extreme interest to researchers and technologists. Optoelectronics is a technology that uses electronic circuitry to not only produce but to detect and control the photonic signals. Being a very quickly growing technology, it is used in most of the devices and appliances available around us. A few examples include cameras, light emitting diodes (LED), display units, sensors, optical memories, optical communication systems, clinical equipment, etc. The opto-electronical behaviour of crystals depends on various factors such as intermolecular interactions, packing arrangements, molecular orientations and molecular structures. In an optoelectronic material, the existence of a hydrogen bond, halogen bond and π–π interaction governs the growth habits and hence the crystal properties [1]. On the same line, the intermolecular interactions and molecular structures direct the packing arrangement within the crystal and influence the optoelectronic nature of the material. Molecular orientation of the molecule directly

contributes to the electrical behaviour and photonic property of the material. The dipole moment orientation, with respect to the electric component of light to which the material is exposed, stimulates the emission and absorption parameters of its optical behaviour. Intermolecular interactions, packing arrangements, molecular orientations and molecular structures correlatively control each other and contribute to the resultant opto-electronical nature of the material.

As organic and inorganic compounds possess diverse intramolecular interactions, these materials offer different optical as well as electrical and electronical characteristics. It is reported that a single crystal of an inorganic compound can be easily grown to a bulk size. It has high mechanical strength and a high degree of chemical inertness but shows relatively low NLO coefficients with respect to organic crystals. Conversely, organic crystals show large NLO coefficients, high sensitivity, low mechanical strength and are difficult to grow to a bulk size. Over the past few decades, researchers have taken efforts to combine the advantages of the inorganic and organic compounds and have developed a new class of material termed semi-organic crystals. The organic molecules linked by hydrogen bonds, π–π, or van der Waals intermolecular interactions give better optical performance when combined with inorganic salts. They offer better mechanical and electrical properties and are proven ideal for device manufacturing. This technically important class of crystals finds application in a variety of devices such as photodiodes, photovoltaics (or solar cells), photoresistors, light-emitting diodes (LEDs), encoder sensor integrated circuits (ICs), laser diodes, optical fibres, etc., as shown in Figure 1.

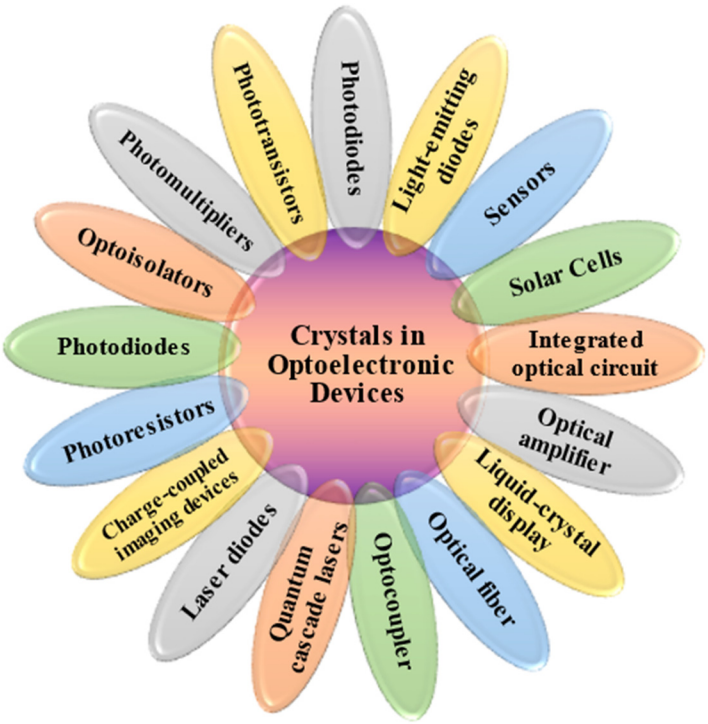

Figure 1. Applications of single crystals in optoelectronic devices.

These varieties of opto-electronical devices work on different principles and hence require various essential properties for individual applications. Researchers around the globe are producing advanced crystals by controlling growth parameters and orientations, morphology, bandgap, charge transport ability, optical sensitivity and electronic transitions. With the same intentions, our goal in the present study is to enhance the optical abilities of the ADP crystal, as its crystalline form has sound applications in the electro-optics industry. For that, an attempt is made to grow L-lysine: ADP single crystals using the SR method, and a detailed report is presented by examining optical (linear and nonlinear), mechanical, and other characteristics. To improve the NLO properties of ADP crystals

intended for commercial usage, an effort was provided in the current experiment to produce large-size ADP crystals with the addition of L-lysine. It should be mentioned that there has not yet been any experimental proof of the impact of the amino acid molecule L-lysine on the development, structural, NLO and mechanical characteristics of the desired orientation on ADP crystals. Several complimentary techniques, including XRD, EDX, optical spectroscopy, FTIR, Vickers microhardness and second harmonic generation, were used to characterize the produced crystals.

2. Ammonium Dihydrogen Phosphate as an Optical Crystal

Ammonium dihydrogen phosphate (ADP) and potassium dihydrogen phosphate (KDP) crystals are grown in sufficient sizes for a variety of technical applications. Comparatively, ADP crystals have greater appeal because of their piezoelectric nature [2]. Because of distinctive nonlinear optical, dielectric and antiferroelectric properties, ADP crystals have attracted the attention of researchers [3]. For Nd: YAG and Nd: YLF lasers, as well as for electro-optical technology such as Q-switches for Ti: Sapphire and Alexandrite lasers and acousto-optical applications, ADP crystals are frequently utilized as the second, third and fourth harmonic generators. ADP ($NH_4H_2PO_4$), in contrast to KDP (KH_2PO_4), has additional N-H-O hydrogen bonds that link PO_4 tetrahedra with the nearby NH_4 group. Two different types of bonds, (O-H-O) and (O-N-H), link each oxygen atom to the nearby oxygen atom in the PO_4 ion and the neighbouring nitrogen atom in the NH_4 ion, respectively (N–H–O). As determined by the X-ray diffraction study's positional refinements of every atom in ADP [4], each NH_4 ion at the potassium location in the KDP structure is moved to an off-centre position both above and below the phase transition point by making two shorter and two longer bonds to four PO_4 tetrahedra in the low-temperature phase. The other proton of the O-H-O bond prefers to stay away from oxygen when it relates to the shorter N-H-O bond; however, with a longer N-H-O bond, the acid proton stays nearby. As a result, at low temperatures, the additional hydrogen bonds disrupt the NH_4 ion lattice and work in conjunction with the acid protons to form proton configurations that are distinct from those observed in KDP at low temperatures [5]. ADP has received significant interest in the study of hydrogen bond behaviours in crystals, and the correlation between crystal dynamics and related characteristics.

Numerous researchers have shown vital interest in ADP crystals and various possible doping approaches [6–8]. Several researchers report that the dopant concentration can control the growth parameters of a crystal, in addition to the temperature, saturation of solution and its pH. Additionally, research has been conducted on how additives affect ADP's growth ability, habit modification and structural variations [9–11]. Impurities can adsorb at various places, restrict growth or even block the developing surface. In contrast, the adsorbed impurities might also result in a decline in the edge-free energy, accelerating crystal growth [12]. The number of additives supports the growth mechanism of crystal growth, which in turn leads to a faster growth rate and also qualitatively improves the various physical properties of the grown crystal. This enhanced growth rate and superior quality crystals are reported for the addition of not only organic molecules [13–16] but also inorganic molecules [17–19].

Crystals belonging to the amino acid group have exceptional nonlinear optical and electro-optical characteristics. The literature confirms that amino acid additives in technically significant crystals enhance material nonlinear optics as well as ferroelectric properties. For example, an improvement in optical and thermal stability was reported in L-alanine-doped ADP [20], and an increase in the NLO response of the KDP crystal was seen with the doping of L-arginine [21]. Studies are also available for amino acid additives (L-histidine, L-glutamic acid, L-valine) in KDP [22]. Studying the impact of adding L-threonine, DL-threonine and L-methionine to TGS crystals, the findings revealed that the admixed TGS crystal exhibits distinct features from the pure TGS crystal [23]. L-lysine ($C_6H_{14}N_2O_2$) is one of the promising candidates for producing semi-organic crystals with the aim to be used for nonlinear optical technology [24]. Various properties such as dielectric studies, etching,

NLO, thermal, FTIR and microhardness of L-lysine monohydrochloride dihydrate crystal have been described [25,26], and as with other natural amino acids, L-lysine comprises a proton donor carboxyl acid group (COO^-) and a proton acceptor amino group (NH_3^+). Second-order nonlinearity depends on the molecule's ground state charge asymmetry due to donor and acceptor groups [27].

3. Experimental Procedure

3.1. Crystal Growth

The high-grade purity ADP and L-lysine were applied for growing crystals, employing repeated recrystallization. Deionized water was used as a solvent to grow seed crystals using the slow evaporation method. Based on the solubility information [28], 400 mL of a saturated solution of pure and 0.5 and 1 mol% of L-lysine admixed ADP was prepared, filtered, and the mixture was kept in beakers with a porously sealed cover; the solutions were made to evaporate under the identical circumstances. After nine days, tiny seed crystals were observed in a doped ADP solution and four days later in a pure ADP beaker. Crystals attained a suitable size in almost 20 days. The seed crystals up to size $20 \times 5 \times 15$ mm^3 were harvested. It was observed that the biggest size was attained by the 1 mole % L-lysine: ADP crystal. For growing bulk size unidirectional crystals by an SR method, good quality seed crystals having a size of 10 mm $\times$ 2 mm were chosen. The selected, unpolished seed crystals along the (1 0 0) direction were installed carefully at the base of the vessel [28]. The various growth vessels were carefully filled with the filtered respective solutions of ADP. All the growth ampoules were put in an ultra-clean room with a porously sealed top. For all the ampoules, applied temperatures were maintained at 37 °C at the top, and 33 °C at the bottom, with the help of the temperature controller; the whole setup is illustrated in Figure 2. For L-lysine-added ADP, crystal growth began after five days under ideal conditions, but it took nine days for the growth to begin in pure ADP.

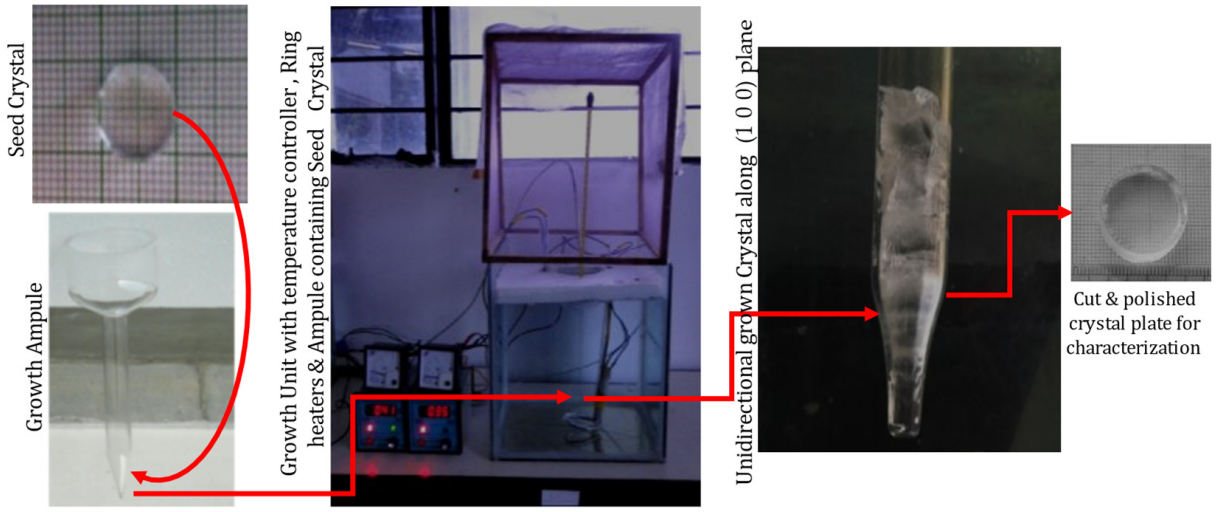

Figure 2. Setup for crystal growth by SR method and the grown crystal.

3.2. Growth Rate

The growth process began in equilibrium conditions with an appropriate temperature maintained with a ring heater in the upper section of the saturated solution. Throughout the entire growth process, the upper ring heater of the solution controls the spurious nucleation in the vicinity of the surface. Extremely translucent crystal formation was witnessed in ideal conditions with a growth rate of about 1.5 mm/day noted for doped crystals; however, for pure ADP, the rate of growth was found to be 1 mm/day only [29]. It was noted that the growth rate was higher for 1 mole % doping of L-lysine than the other two crystals for the 10 mm diameter ampoule. After 30 days, L-lysine-added ADP crystals around a size of

10 mm × 40 mm were harvested. This suggests that L-lysine doping in the mother solution enhances the growth mechanism of the ADP crystal.

ADP crystals include a variety of chemical bonds, but the weaker ones created during crystallization have the strongest effects on crystal building. The fundamental atomic elements approach the crystal during the process of forming crystals in an aqueous solution, and take the structure of primary growth units that are created due to powerful chemical bonds that exist inside them. Throughout the whole crystallization, the bond number and bond strength within the growth units are nearly constant. The bond strength within growth units, which makes up their constituent parts, is often stronger but has minimal effect on the crystallization process. Instead, the weaker chemical bonds that form among growth units throughout the crystallization mechanism ultimately determine how the crystal will grow.

The growth rate is discovered to be affected by impurity doping. This can be explained as follows: the surface concentration of growing species and surface energy may have changed due to the addition of L-lysine, which has a higher solubility than the ADP. L-lysine may boost solubility by reducing the surface energy of the growth stages, which in turn reduces the rate of layer displacement that accelerates the growth process [30]. Urea-doped KDP [31], L-alanine, L-Arginine monohydrochloride (LAHCl) [32] and NH_4Cl [33] doped ADP have reported similar outcomes.

3.3. Characterization

Single crystal X-ray diffraction examinations are performed on all the crystals using a single X-ray diffractometer (Bruker Kappa Apex II), with radiation of wavelength 0.71073 Å in order to estimate the lattice constants and confirm the crystallinity of the grown samples. The powder crystal diffraction pattern was noted using an advanced X-ray diffractometer (Bruker AXS D8 Advance), which was exposed to CuK radiation with a wavelength of 1.54056 Å. The samples were scanned at a rate of 0.02° per second over the required 2θ range of 10–80°. A micro-analytical method called energy dispersive X-ray analysis (EDAX) is utilized to learn more about the crystal's elemental composition. In the present investigation, the crystal's chemical constitution was examined by a JEOL Model JSM–6380A device. The FTIR spectrum of doped and undoped ADP crystal has been studied on a Perkin Elmer Fourier Transform Infrared spectrometer (Model: RXI) in the specific range of 400–4000 cm^{-1} by the KBr pallet system. Phase transition, crystallization, and various stages of the crystal system's decomposition are all subject to information provided by thermogravimetric analysis (TGA) and differential thermal analysis (DTA) over a temperature range of 28–800 °C in the nitrogen atmosphere, using an instrument Perkin Elmer Diamond with alumina as the reference. The 2 mm thick grown crystal plates were sliced and used for optical experiments. These plates had not been applied with an antireflection coating. Using a Varian, Cary 5000 UV-Visible Spectrophotometer, the UV–visible–near-IR transmission spectra were captured between 200 nm and 1200 nm. A hardness study of the grown crystals over the face (1 0 0) has been carried out and is reported. For the microhardness study, the grown crystals' appropriate size was chosen. Vicker's indenter was used to make indentations under various loads. A number of indentations were performed for every single load (p), and the average diagonal length (d) was used to determine the crystals' microhardness. $Hv = 1.8544p/d^2$ was used to evaluate Vicker's microhardness number. The Kurtz and Perry powder method was implemented to investigate the grown crystals' second harmonic generation [34]. A Q-switched Nd: YAG laser operating at a wavelength of 1064 nm, with incoming pulse energy of 1.9 mJ/pulse, a pulse width of 8 ns, and a repetitive rate of 10 Hz, was used to perform the SHG analysis on the salts of pure and L-lysine-added ADP. The green emission of the powdered samples, which was collected at the output, demonstrated that all ADP crystals behaved nonlinearly.

4. Result and Discussions

4.1. Single Crystal X-ray Diffraction Analysis

The crystallinity and structural characteristics can be investigated using single crystal X-ray diffraction examinations. Table 1 depicts the lattice constant reported in this study.

Table 1. Cell parameters of ADP crystals from Single Crystal XRD study.

Crystals	Lattice Parameters		Volume V (Å^3)	Interfacial Angles
	a = b (Å)	c (Å)		
Pure ADP	7.510	7.654	431.68	$\alpha = \beta = \gamma = 90^\circ$
0.5% L-Lysine-doped ADP	7.4979	7.5348	423.60	$\alpha = \beta = \gamma = 90^\circ$
1% L-Lysine-doped ADP	7.4947	7.538	423.41	$\alpha = \beta = \gamma = 90^\circ$

The lattice constants obtained in this study for grown ADP crystals are in fair agreement with those obtained by earlier authors [35]. It is observed that the lattice dimensions of these crystals belong to tetragonal unit cells that pertain to space group I42d. These samples employ a single phase and show very feeble variation in lattice constants for doped crystals. However, the differences in the lattice volumes between undoped and doped ADP samples observed in the present work are too small to create any lattice distortion in the ADP crystal. This observation confirms that the inclusion of lysine molecules has been incorporated into the crystal lattice but has not distorted the basic lattice of the ADP crystal. The lattice constants increase when the rate of impurity molecule adsorption is low as compared to the rate of deposition of the growth entities, while the lattice parameters may shorten when the rate of impurity molecule adsorption is fast compared to the rate of accumulation of the growth entities. This fast absorption rate of impurity is further confirmed by the increased rate of growth for dopped ADP crystals compared to pure crystal, discussed in detail in the next section. In ADP crystal, the addition of L-lysine causes a decrease in lattice parameters, and it is also seen that with an increase in impurity concentration, only a slight variation in the volume of the crystal is observed.

4.2. Powder XRD Analysis

The diffraction pattern of pure ADP crystals depicts the perfect matching with JCPDS card number 89–7401, shown in Figure 3. The XRD pattern confirms the tetragonal structure for all the grown samples with space group I-42d. As in the diffraction spectra of the doped ADP, the crystal exhibits no additional peaks, indicating no record of any additional phase besides the tetragonal system. The crystallinity of the produced crystals is confirmed by the sharpness of the peaks. The development of isolated centres of NH_4^+ in the crystal lattice may be the cause of the improved crystallinity in the L-lysine-supplemented ADP; it hinders the production of bivalent ions' chain structures [36].

The comparison of unit cell dimensions confirms the contraction of lattice dimensions and hence cell volume with an increase in doping concentration. Further, variations in peak intensities are noted for all the grown single crystals. In the case of doped ADP crystals, the highest intensity is shifted to the (112) peak, whereas the pure ADP crystal's highest peak is at the (200) plane. This shift in peak intensity to the (112) plane must be due to the incorporation of the L-lysine molecule near that plane [37]. The lattice dimensions and spacing are obtained from the XRD study, and the data evaluated are listed in Table 2.

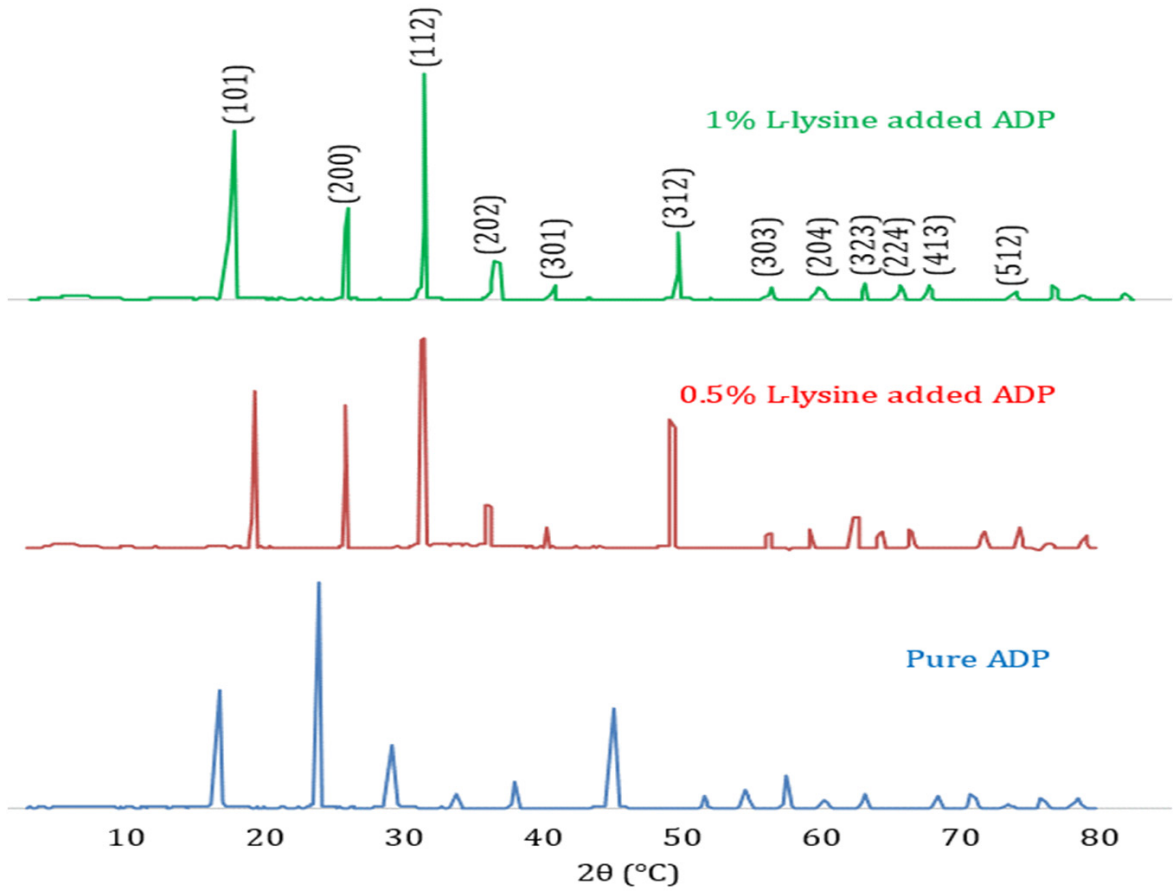

Figure 3. Comparative X-ray Diffraction Pattern of pure and doped ADP crystals.

Table 2. Cell parameters and interplanar spacing of pure and doped ADP single crystal.

Crystal	a = b (Å)	c (Å)	d_{101} (Å)	d_{200} (Å)	d_{112} (Å)	d_{202} (Å)	d_{301} (Å)	d_{312} (Å)	d_{303} (Å)
Pure ADP	7.5116	7.5795	5.3355	3.7554	3.0849	2.6676	2.3774	2.0126	1.7784
0.5% L-Lysine-doped ADP	7.4911	7.5786	5.3276	3.7455	3.0819	2.6638	2.3716	2.003	1.7758
1% L-Lysine-doped ADP	7.4375	7.5273	5.2905	3.7187	3.0606	2.6452	2.3547	1.9945	1.7754

4.3. EDAX Characterization

A micro-analytical method called energy dispersive X-ray analysis (EDAX) is utilized to learn more about the crystal's precursor molecule. The sample is exposed to high-intensity electron radiation during an energy-dispersive X-ray examination to quantify the weight percentage of C, N, P and O, as presented in respective tables. The atomic number of elements contained has an impact on the energy of the radiation that results from it. The intensity and binding energy relation of the photoelectron that was released are recorded in the EDAX spectrum. It is noteworthy that the measurements of the number of constituents available in the sample are shown by peak height and peak area in Figure 4.

The elements carbon, nitrogen, oxygen and phosphorous are found in the grown crystal sample indicated by the corresponding energy peak. The energy peaks obtained in the EDAX spectrum of the element are given as oxygen 0.525 keV, phosphorous 2.013 keV, nitrogen 0.392 keV and carbon 0.277 keV. The presence of carbon validates the incorporation of amino acid molecules in doped crystals, which is also verified from the XRD data.

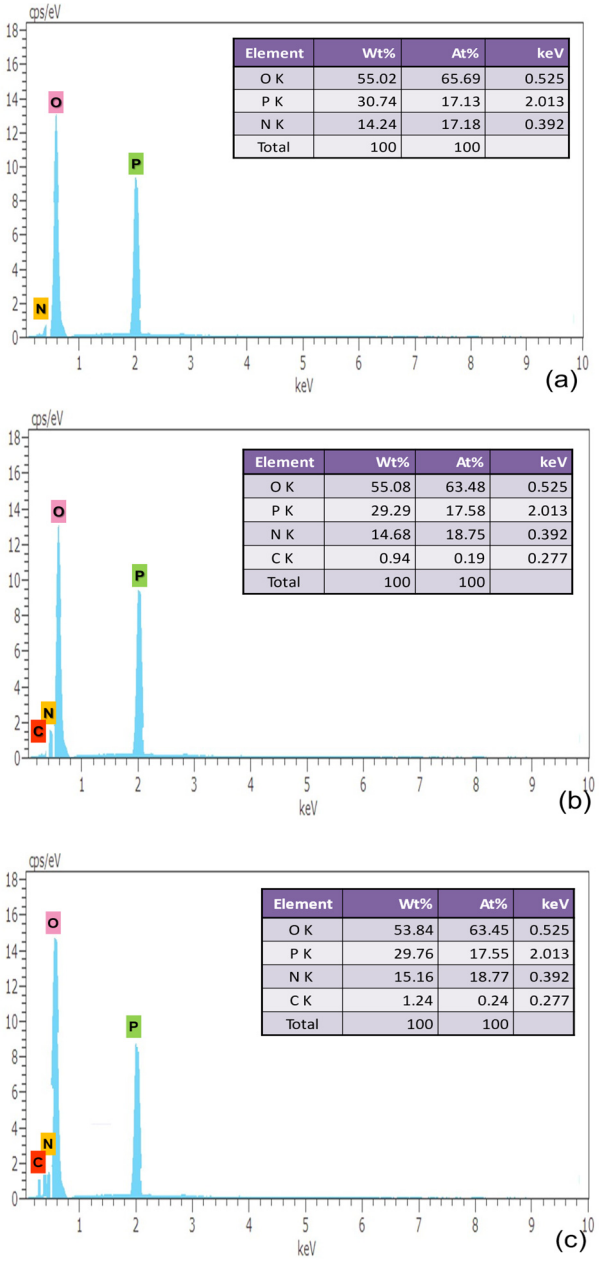

Figure 4. EDAX Characterization of (**a**) pure, (**b**) 0.5% L-Lysine and (**c**) 1% L-Lysine-doped ADP.

4.4. FTIR Analysis

FTIR spectra of all the grown ADP crystals were recorded and are plotted in Figure 5. The O-H vibrations of water, the P-OH group, and the N-H bond vibrations of ammonium are responsible for the broadband in the high energy area [33]. The hydrogen bond interaction of nearby molecules causes the band's broadness [38]. The combination of band vibrations at 1281 and 1089 cm^{-1} causes the peak at 2379 cm^{-1}. The peak at 1646 cm^{-1} is caused by water bending vibrations. The bending vibration of ammonium is what causes the peak at 1402 cm^{-1} [39]. The P-O-H vibrations produce the 1092 cm^{-1} and 932 cm^{-1} peaks. The peaks for the PO_4 vibrations are at 544 and 470 cm^{-1}.

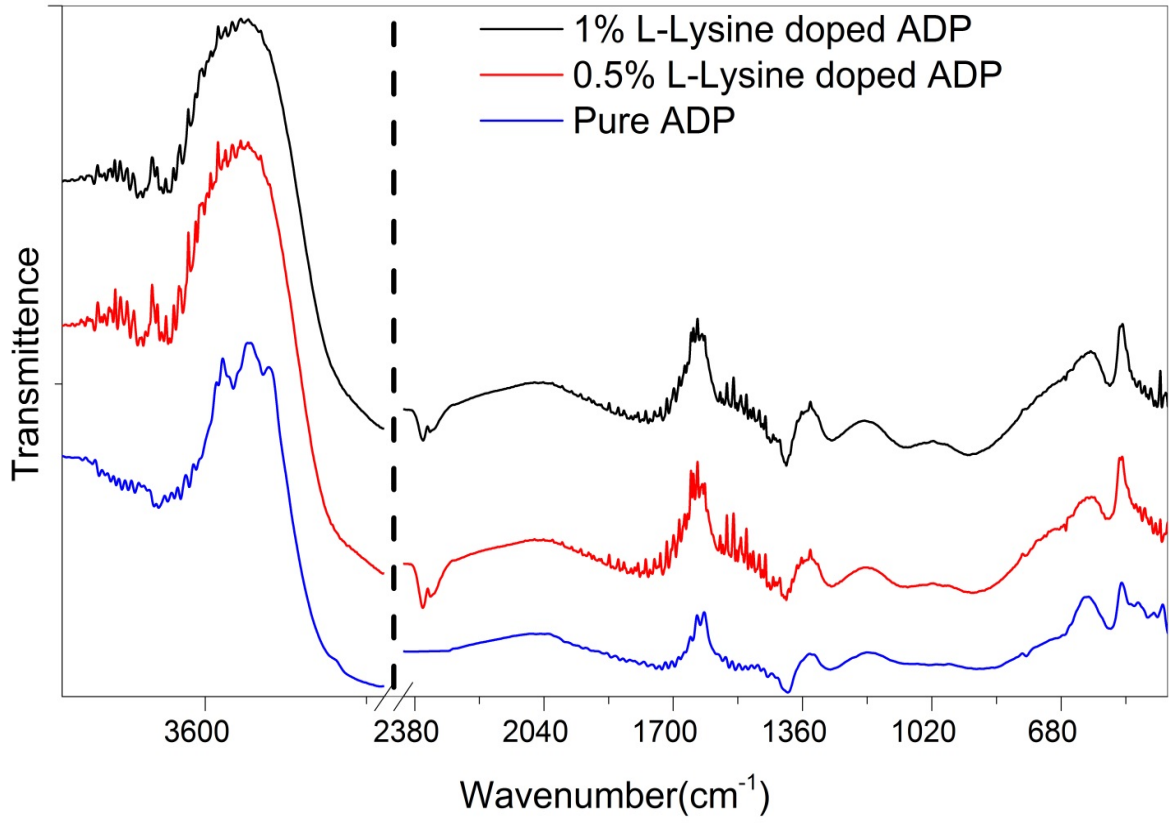

Figure 5. FTIR of grown ADP crystals.

All functional groups are tabulated in Table 3 and indicate the shift in absorption wave number, owing to changes in the bond lengths of the O-H and P=O bonds. In addition, the weak force of attraction between the O-H and P=O bonds governs the optical properties of the ADP crystal. This force of attraction may possibly originate from the presence of the NH_4^+ ion in the tetragonal ADP crystal lattice, which is in good agreement with the results previously reported in a few studies [40].

Table 3. FTIR of pure and doped ADP.

SN	Functional Group	Pure ADP cm^{-1}	0.5% L-Lysine Doped ADP cm^{-1}	1% L-Lysine Doped ADP cm^{-1}
1	O–H stretch of water	3403	3406	3407
2	N–H stretching	3223	3227	3229
3	O=P-OH stretching	2379	2380	2382
4	O-H bending	1706	1713	1714
5	O-H bending vibrations of water	1642	1646	1647
6	Asymmetric mode of—COO and CQC stretching	—-	1569	1569
7	Symmetric mode of—COO and C–N stretching	—-	1417	1418
8	Bending vibration of ammonia	1409	1409	1411
9	P-O-H asymmetric stretching	1092	1091	1092

Table 3. *Cont.*

SN	Functional Group	Pure ADP cm^{-1}	0.5% L-Lysine Doped ADP cm^{-1}	1% L-Lysine Doped ADP cm^{-1}
10	C–O stretching of carboxyl group	—-	1089	1091
11	O–H stretching of carboxylic acid	—-	1000	1000
12	P-O-H asymmetric stretching	910	913	914
13	PO_4 vibrations	544	546	546
14	PO_4 vibrations	470	470	470

4.5. Thermal Analysis

Thermal stability and decomposition temperature of the harvested crystals were investigated by means of thermogravimetric analysis (TGA) and differential thermal analysis (DTA), which provide details on crystallization, phase transition and various stages of crystal system disintegration. TGA curves for all the grown specimens are shown in Figure 6. The curves were obtained for the temperature range between room temperature (28 °C) and 800 °C in a nitrogen atmosphere.

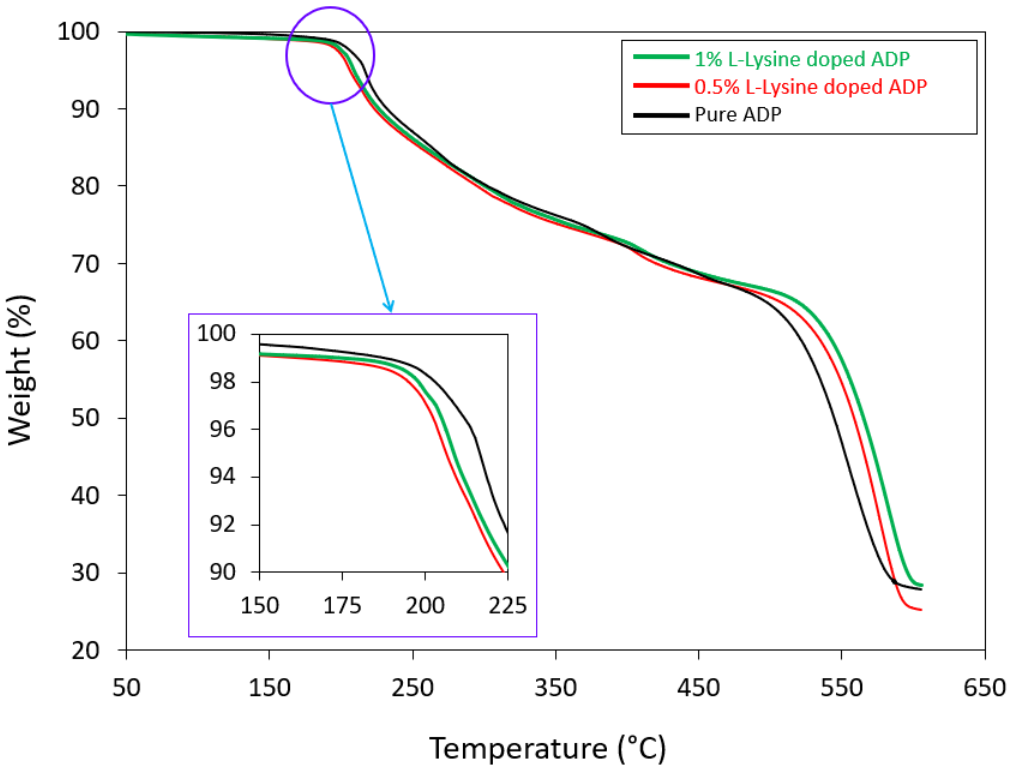

Figure 6. TGA curves of grown crystals.

The TGA trace represents the decomposition temperature of the crystals. The initial decomposition brought on by water molecule dehydration occurs at 195.2 °C and 196.7 °C for 0.5 and 1 mole % doped crystals, respectively, whereas, for pure ADP, the starting decomposition temperature is 197.1 °C. After this temperature for all the crystals, a consistent loss of weight is seen (nearly 64%), approximately 535 °C, reflecting continuous decomposition of the material. Above 600 °C, decomposition reaches its final state, reflecting a maximum loss of around 80% for pure and all doped crystals. The doped crystals show a slightly higher rate of weight loss compared to the pure ADP crystal.

The DTA of all the grown crystals was performed at the temperature range between 28 °C and 600 °C. The DTA traces shown in Figure 7 indicate a strong endothermic peak

between 201 °C and 204 °C for doped crystals, whereas for pure ADP crystal, it is at 214 °C. These peaks correspond to the melting of the crystals. Hence, the DTA curve reveals that the thermal stability of the L-lysine: ADP crystal is slightly hindered in comparison to the pure ADP crystal. It can also be concluded that with the increase in impurity concentration, the thermal stability of crystals decreases. The incorporation of the L-lysine molecule in the ADP crystal matrix may lead to an increase in bond order, which is inversely proportional to the bond length. In addition, the enhanced growth rate of doped crystals due to the fast absorption rate of impurity molecules may incorporate defects within. The inclusion of defects and a decrease in bond length leads to a decrease in thermal stability. A similar nature was noted for L-lysine-doped KDP [41] and L -LMHCl dihydrate-doped ADP [42].

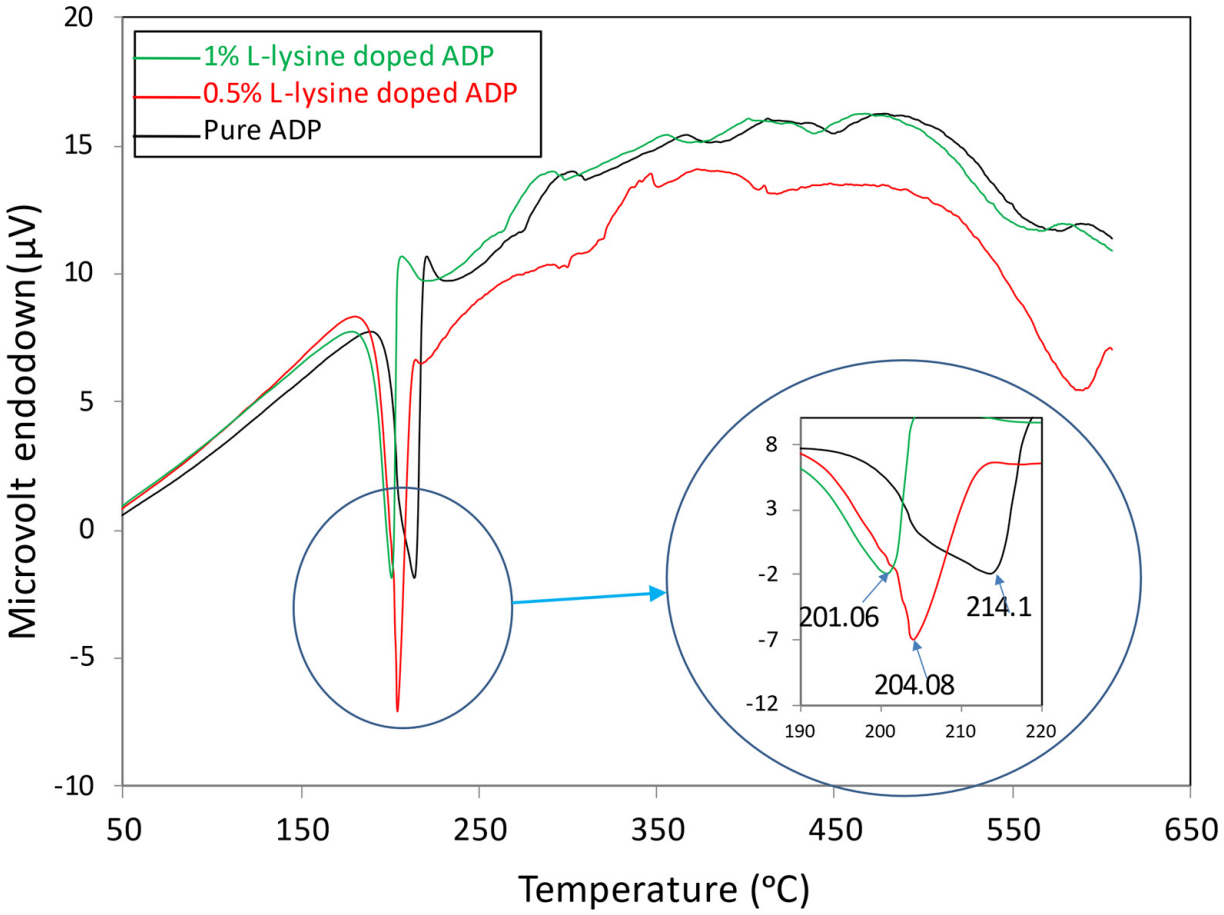

Figure 7. DTA curves of grown crystals.

4.6. UV–Vis-NIR Analysis

The linear optical characterization is primarily used to estimate the optical transmission window and cut-off wavelength for any given sample. ADP crystals find their prime applications in optical industries; thus, it becomes necessary to carry out optical transmission studies. Figure 8 depicts the UV–Visible–near-IR transmission curve for grown crystals in the range of 200 nm to 1000 nm.

It was seen from the spectra that the produced ADP crystals displayed good transmittance over the wide window and hence found their application in UV-tuneable lasers and frequency conversion devices [43,44]. L-lysine has improved the optical quality of the ADP crystal, as is evident from the overlay UV–Vis–IR spectra, giving higher transmittance for 1% L-lysine: ADP crystal (~87%). This is due to the fact that in complexes involving metal and organic coordination, the organic legend dominates the NLO effects. The amino acids possess higher transmittance when added to ADP, resulting in an increase in transmittance. It may be due to the interaction between the O–H and C=O bonds [45]. Hence, it can be

concluded that the organic L-lysine molecule increases the optical transparency of the ADP crystal, which is in good agreement with the results reported earlier [46–48]. Additionally, the purity of the starting materials and higher crystalline perfection play important roles in transmittance. The optical cut-off wavelength for pure and doped crystals ranges from 214 to 220 nm.

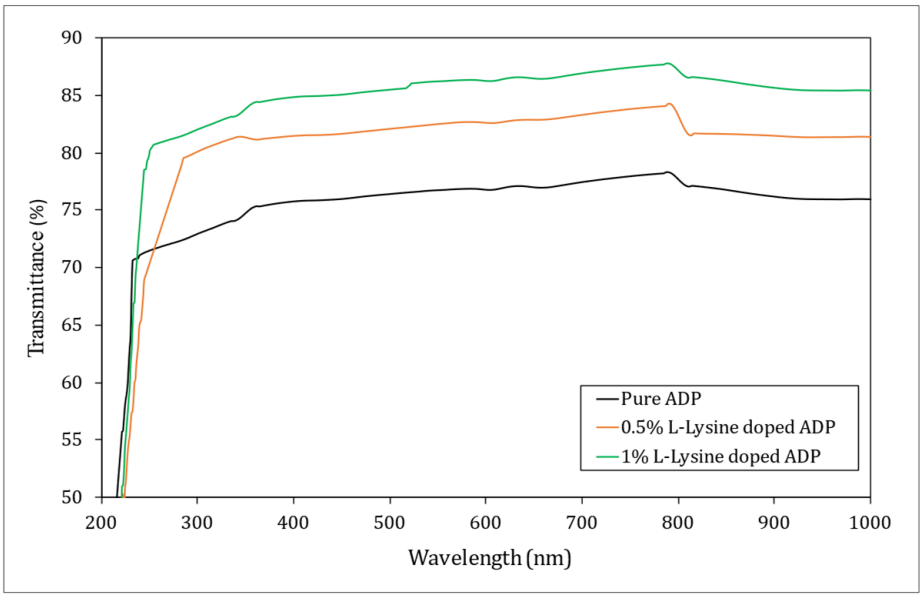

Figure 8. UV–Vis transmission spectrum of ADP crystals.

The linear absorption coefficient is an important parameter to consider when dealing with the propagation of electromagnetic radiation in a crystalline material. During the path of the radiation, each photon interacts with the constituent molecules encountering them, and the number of interactions increases with an increase in the density or the thickness of the sample [49]. The relation between absorption coefficient (α) and photon energy (hν) is given by

$$(\alpha h\nu)^2 = A\ (h\nu\text{-}Eg) \quad (1)$$

Here, A represents constant, and Eg is band gap Energy. To measure the absorption coefficient, the Tauc plot in between '$(\alpha h\nu)^2$' and 'hν' is plotted in Figure 9, and it is calculated by using the formula

$$\alpha = \ln(1/T)/t \quad (2)$$

where T is transmittance, and t is the thickness of the crystal under test, which is equal to 2 mm in this case. The Tauc plot, shown in Figure 9a,b, gives the value of direct and indirect band gap energy. The direct Eg estimated from the Tauc curve is found to vary from 5.1 to 5.2 eV for grown crystals sufficient for optoelectronic devices, and the indirect band gap is found to be in the range of 4.1 eV to 4.4 eV; it is highest for 1% L-lysine-added ADP crystal, proving it to be suitable for optical devices [43,50].

4.7. Vickers's Microhardness Analysis

For many applications, good quality crystals with improved optical features and enhanced mechanical strength are required. The hardness parameter of the grown ADP crystal was measured for the dominant face (1 0 0), and a plot of hardness value against accompanying loads is presented in Figure 10.

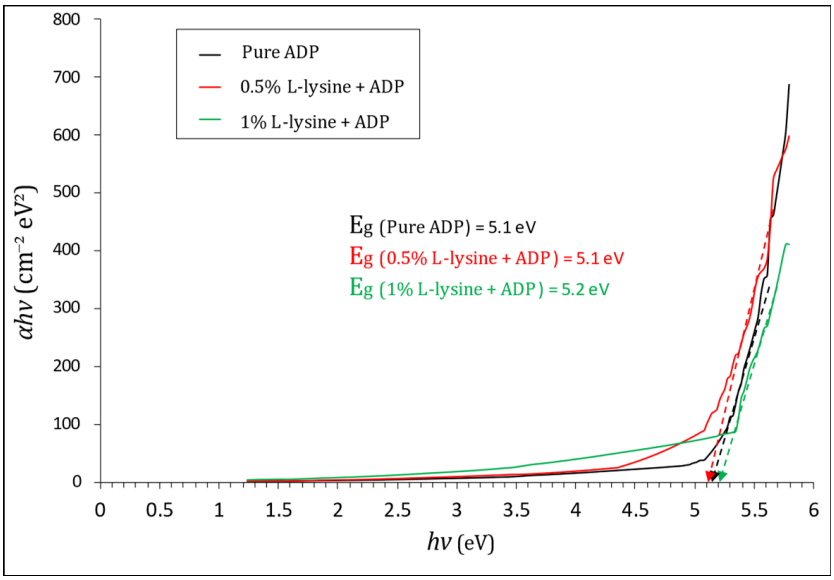

(**a**)

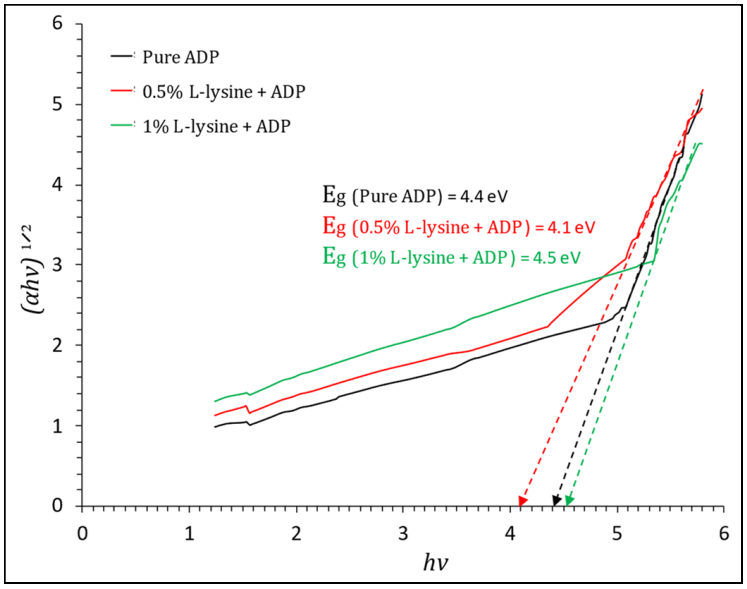

(**b**)

Figure 9. (**a**). Tauc plot of $(\alpha h\nu)^2$ vs. hν and evaluation of direct optical band gap for pure and doped ADP. (**b**). Tauc plot of $(\alpha h\nu)^{1/2}$ vs. hν and evaluation of indirect optical band gap for pure and doped ADP.

The hardness curve reflects that the L-lysine-added ADP crystal has increased hardness compared to the undoped ADP crystal. Hence, the addition of L-Lysine in ADP has provided mechanical strength to the lattice of the ADP crystal; the same results are reported in L -LMHCl dihydrate-doped ADP [42]. In the same way, it is noticed that with an increase in the doping percentage of L-lysine, the hardness of the crystal also increases. This can be correlated with the observations of the XRD study, which shows a decrease in the volume of the crystal lattice for the doping of L-lysine. The reduction in volume corresponds to minimum surface energy and hence a more stable lattice; as a result, crystals offer higher mechanical strength compared to pure ADP [51]. It is also noticed that up to 100 gm, no cracks have been observed in doped crystals.

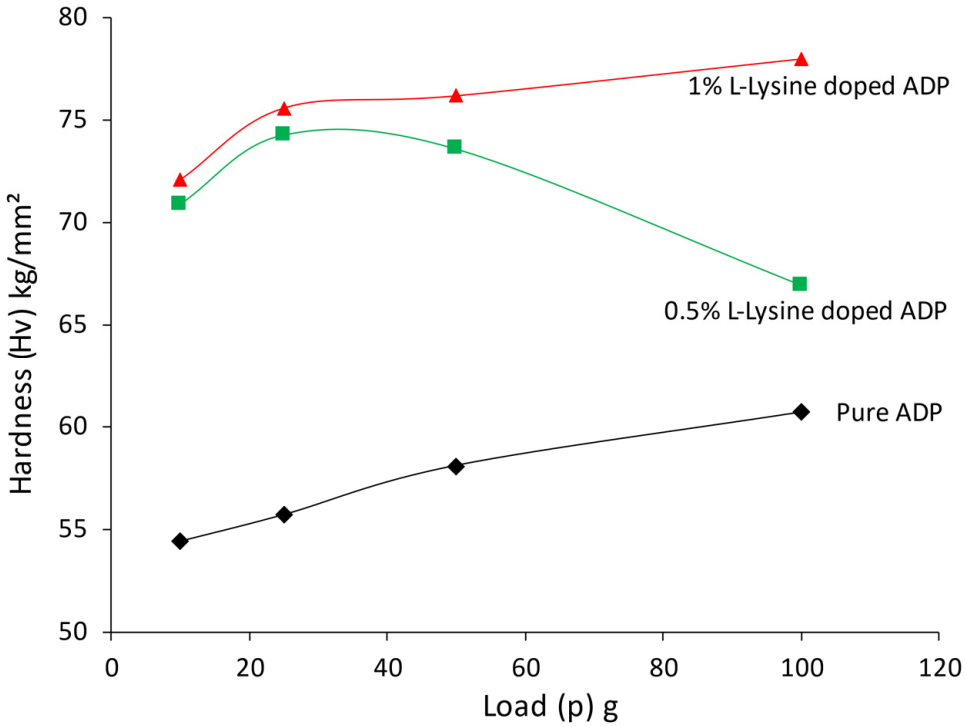

Figure 10. Variation of H_v factor with load for ADP crystals.

4.8. SHG Analysis

In order to evaluate the efficacy of the crystal to be used in NLO-assisted photonics applications, the grown samples are subjected to the SHG test. Second harmonic generation (SHG) is nothing but the nonlinear optical phenomenon, where the interaction of a photon with nonlinear material facilitates the same frequency photon to effectually combine and produce a photon with two-fold the frequency and half the wavelength of the original photons [52]. In the present study, the nonlinear response of grown crystals is tested by the Kurtz–Perry technique. It is the method basically employed for the estimation of second-order nonlinear susceptibility of a sample using the phenomenon of SHG. Here, in this test, a beam of laser with a certain fixed frequency is made to an incident on the sample under the test, and, at the output window, the double of incident frequency captured reveals the NLO behaviour of the material.

In the present findings, all the obtained crystals were crushed to obtain micro granules of the size 125–150 mm so as to be greater than the coherence length of radiation used for the test; the fine powder was then filled in a microcapillary of a uniform bore for further photo exposure [14]. On exposing the sample to the radiation of wavelength 1064 nm, the green emitted radiation confirms the nonlinear nature of all ADP crystals. The whole setup and all the related parameters were set to a similar setting for all samples to attain a relative comparison of SHG efficiency. The output signal is recorded via a photomultiplier tube, which produces an electrical signal proportional to the intensity of the detected signal. In addition, finally, the digital oscilloscope displays the corresponding recorded SHG voltage. The output voltage for the pure ADP sample was obtained as 86 mV, whereas, for 0.5 and 1% L-Lysine-doped ADP, the voltages were 94 mV and 132 mV, respectively. Considering ADP as a reference material, the SHG efficiencies of doped ADP crystals are compared in Table 4. The enhanced nonlinear response is observed for doped crystal due to the presence of the amino acid molecule in the ADP crystal matrix [53,54].

Table 4. SHG efficiency.

SN	Crystals	SHG (Signal) mV	Efficiency w. r. t. ADP
1	Pure ADP	86	1
2	ADP doped with 0.5% L-Lysine	94	1.09
3	ADP doped with 1% L-Lysine	132	1.53

For the material to exhibit second-order nonlinearity, the compound matrix must possess a non-centrosymmetric structure. In organic compounds, the linear and nonlinear behaviour reflects an anisotropic nature. Amino acid compounds consists of proton contributor carboxylic acid (–COO) assembly and proton acceptor amino (–NH2) assembly. This type of molecular structure facilitates the second harmonic generation, forming dipole–dipole orientations of H-bonded chiral molecules, which gives non-zero, first-order hyperpolarizability [55]. Additionally, amino acids radially support the structural changes that contribute to the rise in NLO behaviour. In the ADP: L-lysine compound, upon interaction with highly intense electromagnetic radiation, the response of constituent molecules is very expressive due to an acentric structural orientation, and the strong delocalization tendency of charges results in a more polarized molecule [56,57]. In the ADP crystal matrix, the PO_4 group's contribution to the SHG impact is predominant. The probability of a hydrogen bond forming between the amino group of L-lysine and the oxide of the phosphate group of the ADP matrix may boost the contribution of PO_4 to the SHG response. Additionally, the hydrogen bond and carbonyl group are incorporated into the ADP crystal due to the addition of amino acids, which may help to increase the SHG characteristic [58,59]. In addition, in L-Lysine, there is more dipole movement due to the presence of the polar NH_3 amino group. When L-Lysine reacts with ADP, the optically active amino group tends to replace some ammonium ions and increases its non-centrosymmetry; this may lead to an increase in intermolecular charge transfer, which in turn gives rise to the nonlinearity of the crystal [60]. Hence, the L-Lysine-doped ADP crystal shows a large SHG efficiency. This confirms that the admixing of organic amino acid enhances the nonlinear response of crystal ADP [61].

5. Conclusions

Single crystals of ADP (pure and L-lysine-added) were obtained in a temperature-controlled environment using the S-R method. The growth direction was selected to be along the [1 0 0] plane for all crystals. Throughout the growth process, the growth parameters were closely monitored for all the crystals, which suggest that the addition of an L-lysine molecule enhances the rate of growing and is directly proportional to the doping concentration. Single crystal XRD and powder XRD confirm the tetragonal crystal structure pertaining to the space group I42d. The chemical compositions of all the crystals were analysed by an EDAX study. The presence of carbon in doped crystals proves the incorporation of the impurity in the crystals. The functional group of material was examined by an FTIR analysis. Further studies show that thermal stability tends to decrease for doped crystals. This may be due to a decrease in bond strength and the inclusion of defects in the crystal upon the addition of L-lysine to the ADP lattice. At the same time, the doped crystals show higher transmittance due to the presence of an optically active amino acid group, which proves that ADP: L-lysine crystals are good optical quality crystals. The direct and indirect band gap estimated show a wide enough forbidden energy gap, which is useful in optical devices. Furthermore, the mechanical strength of the crystals was improved by the presence of organic doping. Moreover, the nonlinear property of the ADP crystal confirms the enhancement of the NLO efficiency with doping due to the incorporation of the carboxylic group in the crystal assembly. The molecular interaction of the amino acid and the phosphate group of ADP with electromagnetic radiation is the primary cause of improved SHG behaviour. Hence, it can be concluded

that linear and nonlinear optical properties as well as the mechanical strength of crystals improve with the addition of an L-lysine molecule to the ADP crystal, making it a more efficient candidate for opto-electronic applications such as nonlinear frequency conversion or tuneable laser applications.

Author Contributions: Conceptualization, S.P.; Methodology, S.P.; Experimentation, S.P.; Data curation, S.P. and D.R.; Formal analysis, S.P.; Writing—original draft, S.P. and D.R.; Visualization, D.R.; Validation, D.R.; Project administration, D.R. and K.R.; Supervision, K.R. All authors have read and agreed to the published version of the manuscript.

Funding: This research received no external funding.

Institutional Review Board Statement: Not applicable.

Informed Consent Statement: Not applicable.

Data Availability Statement: The data presented in this study are available on request from the corresponding author.

Conflicts of Interest: The authors declare no conflict of interest.

References

1. Yu, P.; Zhen, Y.; Dong, H.; Hu, W. Crystal engineering of organic optoelectronic materials. *Chem* **2019**, *5*, 2814–2853. [CrossRef]
2. Takubo, H.; Makita, H. Refractometric studies of $NH_4H_2PO_4$ and KH_2PO_4 solution growth; experimental setup and refractive index data. *J. Cryst. Growth* **1989**, *94*, 469–474. [CrossRef]
3. Gunning, M.J.; Raab, R.E.; Kucharczyk, W. Magnitude and nature of the quadratic electro-optic effect in potassium dihydrogen phosphate and ammonium dihydrogen phosphate crystals. *J. Opt. Soc. Am. B* **2001**, *18*, 1092–1098. [CrossRef]
4. Srinivasan, K.; Meera, K.; Ramasamy, P. Enhancement of metastable zone width for solution growth of potassium acid phthalate. *J. Cryst. Growth* **1999**, *205*, 457–459. [CrossRef]
5. Matsushita, E.; Matsubara, T. The role of hydrogen bonds in antiferroelectricity of $NH_4H_2PO_4$. *J. Phys. Soc. Jpn.* **1987**, *56*, 200–207. [CrossRef]
6. Zaitseva, N.; Carman, L. Rapid growth of KDP-type crystals. *Prog. Cryst. Growth Charact. Mater.* **2001**, *43*, 1–118. [CrossRef]
7. Ren, X.; Xu, D.; Xue, D. Crystal growth of KDP, ADP, and KADP. *J. Cryst. Growth* **2008**, *310*, 2005–2009. [CrossRef]
8. Pavithra, K.; Rajesh, P. Effect of zinc acetate dihydrate on the crystal growth, structural, optical, mechanical, dielectric, and NLO properties of ammonium dihydrogen phosphate single crystals. *J. Mater. Sci. Mater. Electron.* **2022**, *33*, 24677–24689. [CrossRef]
9. Davey, R.J.; Mullin, J.W. Growth of the {100} faces of ammonium dihydrogen phosphate crystals in the presence of ionic species. *J. Cryst. Growth* **1974**, *26*, 45–51. [CrossRef]
10. Boukhris, A.; Souhassou, M.; Lecomte, C.; Wyncke, B.; Thalal, A. Evolution of the structural and mean square displacement parameters in solid solutions versus concentration and temperature. *J. Phys. Condens. Matter* **1998**, *10*, 1621. [CrossRef]
11. Mahadik, A.; Mithani, A.; Chaudhari, K.; Soni, P.H. A temperature dependence study of dielectric behaviour and conductivity of pure and L-Leucine doped potassium dihydrogen phosphate (KDP) crystals. *J. Mater. Sci. Mater. Electron.* **2022**, *33*, 25551–25566. [CrossRef]
12. Rak, M.; Eremin, N.N.; Eremina, T.A.; Kuznetsov, V.A.; Okhrimenko, T.M.; Furmanova, N.G.; Efremova, E.P. On the mechanism of impurity influence on growth kinetics and surface morphology of KDP crystals—I: Defect centres formed by bivalent and trivalent impurity ions incorporated in KDP structure—Theoretical study. *J. Cryst. Growth* **2005**, *273*, 577–585. [CrossRef]
13. Kern, R.; Dassonville, R. Growth inhibitors and promoters examplified on solution growth of paraffin crystals. *J. Cryst. Growth* **1992**, *116*, 191–203. [CrossRef]
14. Bhagavannarayana, G.; Kushwaha, S.K. Enhancement of SHG efficiency by urea doping in ZTS single crystals and its correlation with crystalline perfection as revealed by Kurtz powder and high-resolution X-ray diffraction methods. *J. Appl. Crystallogr.* **2010**, *43*, 154–162. [CrossRef]
15. Arasi, M.A.; Alagar, M.; Punyawudho, K.; Pugalenthi, M.R.; Gayathri, R.; Shah, A.A.; Okonkwo, P.C. Influence of glycine and ammonium dihydrogen phosphate on their growth and characterization of l-Alanine single crystal for nonlinear optical applications. *Opt. Mater.* **2022**, *133*, 112992. [CrossRef]
16. Raju, M.M.; Altayran, F.; Johnson, M.; Wang, D.; Zhang, Q. Crystal structure and preparation of Li7La3Zr2O12 (LLZO) solid-state electrolyte and doping impacts on the conductivity: An overview. *Electrochem* **2021**, *2*, 390–414. [CrossRef]
17. Shantha, K.; Philip, S.; Varma, K.B.R. Effect of KCl addition on the microstructural and dielectric properties of bismuth vanadate ceramics. *Mater. Chem. Phys.* **1997**, *48*, 48–51. [CrossRef]
18. Podder, J.; Ramalingom, S.; Kalkura, S.N. An investigation on the lattice distortion in urea and KCl Doped KDP single crystals by X-ray diffraction studies. *Cryst. Res. Technol. J. Exp. Ind. Crystallogr.* **2001**, *36*, 549–556. [CrossRef]
19. Akilandeswari, S.; Jothi, L.; Elkhatib, W.F.; Fayad, E.; Abu Ali, O.A.; El-Sayyad, G.S. Synthesis, spectroscopic, optical, thermal and mechanical characterization of nonlinear proline oxalate single-crystals. *Opt. Quantum Electron.* **2023**, *55*, 14. [CrossRef]

20. Ferdousi, A.; Jiban, P. A Study on structural, optical, electrical and etching characteristics of pure and l-alanine doped potassium dihydrogen phosphate crystals. *J. Cryst. Process Technol.* **2011**, *2011*, 7847.
21. Parikh, K.D.; Dave, D.J.; Parekh, B.B.; Joshi, M.J. Thermal, FT-IR and SHG efficiency studies of L-arginine doped KDP crystals. *Bull. Mater. Sci.* **2007**, *30*, 105–112. [CrossRef]
22. Kumaresan, P.; Babu, S.M.; Anbarasan, P.M. Thermal, dielectric studies on pure and amino acid (L-glutamic acid, L-histidine, L-valine) doped KDP single crystals. *Opt. Mater.* **2008**, *30*, 1361–1368. [CrossRef]
23. Meera, K.; Muralidharan, R.; Tripathi, A.K.; Ramasamy, P. Growth and characterisation of l-threonine, dl-threonine and l-methionine admixtured TGS crystals. *J. Cryst. Growth* **2004**, *263*, 524–531. [CrossRef]
24. Marchewka, M.K.; Debrus, S.; Ratajczak, H. Vibrational spectra and second harmonic generation in molecular complexes of L-lysine with L-tartaric, D, L-malic, acetic, arsenous, and fumaric acids. *Cryst. Growth Des.* **2003**, *3*, 587–592. [CrossRef]
25. Ramesh Babu, R.; Sethuraman, K.; Vijayan, N.; Bhagavannarayana, G.; Gopalakrishnan, R.; Ramasamy, P. Etching and dielectric studies on L-lysine monohydrochloride dihydrate single crystal. *Cryst. Res. Technol. J. Exp. Ind. Crystallogr.* **2006**, *41*, 906–910. [CrossRef]
26. Ramesh Babu, R.; Vijayan, N.; Gopalakrishnan, R.; Ramasamy, P. Growth and characterization of L-lysine monohydrochloride dihydrate (L-LMHCl) single crystal. *Cryst. Res. Technol. J. Exp. Ind. Crystallogr.* **2006**, *41*, 405–410. [CrossRef]
27. Varadarajan, S.; Kumar, M.S.; Shanmugan, S.; Arputhalatha, A.; Chithambaram, V.; Palani, G. A new class single crystal l-lysine hydrogen chloride (LLHC) for optoelectronic applications. *J. Mater. Sci. Mater. Electron.* **2021**, *32*, 26351–26358. [CrossRef]
28. Eimerl, D.; Velsko, S.; Davis, L.; Wang, F.; Loiacono, G.; Kennedy, G. Deuterated L-arginine phosphate: A new efficient nonlinear crystal. *IEEE J. Quantum Electron.* **1989**, *25*, 179–193. [CrossRef]
29. Rajesh, P.; Ramasamy, P. Optical, dielectric and microhardness studies on< 1 0 0> directed ADP crystal. *Spectrochim. Acta Part A Mol. Biomol. Spectrosc.* **2009**, *74*, 210–213.
30. Sangwal, K. Effects of impurities on crystal growth processes. *Prog. Cryst. Growth Charact. Mater.* **1996**, *32*, 3–43. [CrossRef]
31. Pritula, I.; Kosinova, A.; Kolybayeva, M.; Puzikov, V.; Bondarenko, S.; Tkachenko, V.; Tsurikov, V.; Fesenko, O. Optical, structural and microhardness properties of KDP crystals grown from urea-doped solutions. *Mater. Res. Bull.* **2008**, *43*, 2778–2789. [CrossRef]
32. Dhanaraj, P.V.; Bhagavannarayana, G.; Rajesh, N.P. Effect of amino acid additives on crystal growth parameters and properties of ammonium dihydrogen orthophosphate crystals. *Mater. Chem. Phys.* **2008**, *112*, 490–495. [CrossRef]
33. Rajesh, P.; Ramasamy, P. A study on optical, thermal, mechanical, dielectric, piezoelectric and NLO properties of unidirectional ammonium chloride added ammonium dihydrogen phosphate crystal. *Mater. Lett.* **2009**, *63*, 2260–2262. [CrossRef]
34. Kurtz, S.K.; Perry, T.T. A powder technique for the evaluation of nonlinear optical materials. *J. Appl. Phys.* **1968**, *39*, 3798–3813. [CrossRef]
35. Joshi, J.H.; Joshi, G.M.; Joshi, M.J.; Jethva, H.O.; Parikh, K.D. Raman, photoluminescence, and ac electrical studies of pure and l-serine doped ammonium dihydrogen phosphate single crystals: An understanding of defect chemistry in hydrogen bonding. *New J. Chem.* **2018**, *42*, 17227–17249. [CrossRef]
36. Bhagavannarayana, G.; Parthiban, S.; Meenakshisundaram, S. An interesting correlation between crystalline perfection and second harmonic generation efficiency on KCl-and oxalic acid-doped ADP crystals. *Cryst. Growth Des.* **2008**, *8*, 446–451. [CrossRef]
37. Mielniczek-Brzóska, E.; Sangwal, K.; Chocyk, D.; Kluziak, K. Effect of Al (III) impurity on the crystallization of ammonium dihydrogen phosphate (ADP) from aqueous solutions by cooling method. *J. Cryst. Growth* **2022**, *595*, 126816. [CrossRef]
38. Takahashi, M. Terahertz vibrations and hydrogen-bonded networks in crystals. *Crystals* **2014**, *4*, 74–103. [CrossRef]
39. Rani, N.; Vijayan, N.; Riscob, B.; Jat, S.K.; Krishna, A.; Das, S.; Bhagavannarayana, G.; Rathi, B.; Wahab, M.A. Single crystal growth of ninhydrin by unidirectional Sankaranarayanan–Ramasamy (SR) method by using a glass ampoule for nonlinear optical applications. *CrystEngComm* **2013**, *15*, 2127–2132. [CrossRef]
40. Kumari, R.A.; Chandramani, R. Ion transport in Au+ doped/undoped KDP crystals with KI/NaI as additives. *Bull. Mater. Sci.* **2003**, *26*, 255–259. [CrossRef]
41. Parikh, K.D.; Dave, D.J.; Joshi, M.J. Crystal growth, thermal, optical, and dielectric properties of L-lysine doped KDP crystals. *Mod. Phys. Lett. B* **2009**, *23*, 1589–1602. [CrossRef]
42. Rajesh, P.; Ramasamy, P.; Mahadevan, C.K. Effect of L-lysine monohydrochloride dihydrate on the growth and properties of ammonium dihydrogen orthophosphate single crystals. *J. Cryst. Growth* **2009**, *311*, 1156–1160. [CrossRef]
43. Anis, M.; Shirsat, M.D.; Muley, G.; Hussaini, S.S. Influence of formic acid on electrical, linear and nonlinear optical properties of potassium dihydrogen phosphate (KDP) crystals. *Phys. B Condens. Matter* **2014**, *449*, 61–66. [CrossRef]
44. Shaikh, R.N.; Anis, M.; Shirsat, M.D.; Hussaini, S.S. Study on optical properties of L-valine doped ADP crystal. *Spectrochim. Acta Part A Mol. Biomol. Spectrosc.* **2015**, *136*, 1243–1248. [CrossRef]
45. Kumaresan, P.; Babu, B.M.; Anbarasan, P.M. Effect of metal ion and amino acid doping on the optical performance of KDP single crystals. *J. Optoelectron. Adv. Mater.* **2007**, *1*, 65–69.
46. Raghorte, V.R.; Wakde, G.C.; Meshram, N.S.; Rewatkar, K.G. Harvesting amino acid doped KDP crystal by temperature and time control using AVR microcontroller. *Results Chem.* **2020**, *2*, 100074. [CrossRef]
47. Chaki, S.; Deshpande, M.P.; Tailor, J.P.; Chaudhary, M.D.; Mahato, K. Growth and characterization of ADP single crystal. *Am. J. Condens. Matter Phys.* **2012**, *2*, 22–26. [CrossRef]
48. Anis, M.; Shirsat, M.D.; Hussaini, S.S.; Joshi, B.; Muley, G.G. Effect of sodium metasilicate on structural, optical, dielectric and mechanical properties of ADP crystal. *J. Mater. Sci. Technol.* **2016**, *32*, 62–67. [CrossRef]

49. Karuppasamy, P.; Kamalesh, T.; Pandian, M.S.; Ramasamy, P.; Sunil, V.; Chaudhary, A.K. Bulk crystal growth, crystalline perfection and optical homogeneities of 2AP4N single crystals for second and third order frequency conversion and terahertz (THz) device applications. *Opt. Mater.* **2021**, *118*, 111261. [CrossRef]
50. Goel, S.; Sinha, N.; Yadav, H.; Hussain, A.; Kumar, B. Effect of crystal violet dye on the structural, optical, mechanical and piezoelectric properties of ADP single crystal. *Mater. Res. Bull.* **2016**, *83*, 77–87. [CrossRef]
51. Patle, S.; Rewatkar, K. Mechanical Studies of Pure and L-Lysine Doped Ammonium Dihydrogen Phosphate Single Crystal. *J. Adv. Phys.* **2017**, *6*, 379–384. [CrossRef]
52. Liu, X.; Yang, Z.; Wang, D.; Cao, H. Molecular structures and second-order nonlinear optical properties of ionic organic crystal materials. *Crystals* **2016**, *6*, 158. [CrossRef]
53. Muley, G.; Rode, M.; Pawar, B. FT-IR, thermal and NLO studies on amino acid (L-arginine and L-alanine) doped KDP crystals. *Acta Phys. Pol. A* **2009**, *116*, 1033–1038. [CrossRef]
54. Boopathi, K.; Rajesh, P.; Ramasamy, P.; Manyum, P. Comparative studies of glycine added potassium dihydrogen phosphate single crystals grown by conventional and Sankaranaryanan–Ramasamy methods. *Opt. Mater.* **2013**, *35*, 954–961. [CrossRef]
55. Ramesh Kumar, G.; Gokul Raj, S. Growth and physiochemical properties of second-order nonlinear optical L-threonine single crystals. *Adv. Mater. Sci. Eng.* **2009**, *2009*, 704294. [CrossRef]
56. Jazbinsek, M.; Mutter, L.; Gunter, P. Photonic applications with the organic nonlinear optical crystal DAST. *IEEE J. Sel. Top. Quantum Electron.* **2008**, *14*, 1298–1311. [CrossRef]
57. Anis, M.; Muley, G.G.; Hakeem, A.; Shirsat, M.D.; Hussaini, S.S. Exploring the influence of carboxylic acids on nonlinear optical (NLO) and dielectric properties of KDP crystal for applications of NLO facilitated photonic devices. *Opt. Mater.* **2015**, *46*, 517–521. [CrossRef]
58. Jazbinsek, M.; Puc, U.; Abina, A.; Zidansek, A. Organic crystals for THz photonics. *Appl. Sci.* **2019**, *9*, 882. [CrossRef]
59. Parikh, K.D.; Dave, D.J.; Parekh, B.B.; Joshi, M.J. Growth and characterization of L-alanine doped KDP crystals. *Cryst. Res. Technol. J. Exp. Ind. Crystallogr.* **2010**, *45*, 603–610. [CrossRef]
60. Thomas, R.; Pal, S.; Datta, A.; Marchewka, M.K.; Ratajczak, H.; Pati, S.K.; Kulkarni, G.U. Charge density analysis of two proton transfer complexes: Understanding hydrogen bonding and determination of in-crystal dipole moments. *J. Chem. Sci.* **2008**, *120*, 613–620. [CrossRef]
61. Dhanaraj, P.V.; Rajesh, N.P. Effect of Amino Acid Additives on Crystal Growth Parameters and Properties of Ammonium Dihydrogen Phosphate Crystals. In *Crystallization and Materials Science of Modern Artificial and Natural Crystals*; IntechOpen: London, UK, 2012.